Journal of the European Ceramic Society xxx (xxxx) xxx–xxx

Contents lists available at ScienceDirect

Journal of the European Ceramic Society

journal homepage: www.elsevier.com/locate/jeurceramsoc

Short communication

A novel low-temperature firable $La_2Zr_3(MoO_4)_9$ microwave dielectric ceramic

Weiqiong Liu, Ruzhong Zuo*

Institute of Electro Ceramics & Devices, School of Materials Science and Engineering, Hefei University of Technology, Hefei, 230009, PR China

ARTICLE INFO

Keywords:
Microwave dielectrics ceramics
Low-temperature firing
LTCC
Molybdate

ABSTRACT

A novel low-temperature fired $La_2Zr_3(MoO_4)_9$ microwave dielectric ceramic was successfully fabricated by a conventional solid-state reaction method. The powder compact was densified in air in the temperature range of 700–800 °C for 4 h. X-ray diffraction analysis indicated that all studied samples presented a single phase structure. Rietveld refinement results further confirmed that $La_2Zr_3(MoO_4)_9$ belonged to a trigonal system with space group $R\bar{3}c$. Scanning electron microscopy results revealed dense and homogeneous microstructure of $La_2Zr_3(MoO_4)_9$ ceramics as sintered in the temperature range of 725–800 °C. The $La_2Zr_3(MoO_4)_9$ ceramic sintered at 775 °C for 4 h possessed excellent microwave dielectric properties of relative permittivity $\varepsilon_r \sim 10.8$, quality factor Qxf ~ 50,628 GHz (at 10.45 GHz), and temperature coefficient of the resonant frequency $\tau_f \sim -38.8$ ppm/°C, showing great potentials for applications of low temperature co-fired ceramic technology.

1. Introduction

With the rapid development of the microwave communication technology, dielectric ceramics with desirable performances are in great demands [1]. Particularly, the low temperature co-fired ceramic (LTCC) technology has played an increasingly important role in the fabrication of modern electronic devices, which would require dielectric ceramics to have a low sintering temperature to cofirable with Ag, a low permittivity (ε_r) to avoid the signal delay, a high quality factor (Qxf) for better selectivity and a low temperature coefficient of resonant frequency (τ_f) for the frequency stability [2]. Most of conventional microwave dielectric ceramics have good dielectric performances, but their high sintering temperatures restrict their possible applications in LTCC [3,4]. Addition of some low-melting-point aids was considered as a common method to effectively reduce the sintering temperature of dielectric ceramics. However, microwave dielectric properties of the matrix ceramics were seriously degraded in most cases. Thus, searching for new glass-free low-temperature sintered ceramics is essentially important for the development of LTCC technology.

Many Bi_2O_3-, MoO_3-, B_2O_3-, Li_2O- and V_2O_5-based ceramic systems have been in recent years developed for their good dielectric performances and inherently low (ultralow) sintering temperatures [5–13]. For example, $PbMoO_4$ ceramics sintered at 650 °C for 2 h were reported to exhibit microwave dielectric properties of $\varepsilon_r \sim 26.7$, Qxf ~ 42,830 GHz, and $\tau_f \sim +6.2$ ppm/°C [14]. $LiKSm_2(MoO_4)_4$ ceramics sintered at 620 °C for 2 h owned microwave dielectric properties of $\varepsilon_r \sim 11.5$, Qxf ~ 39,000 GHz, and $\tau_f \sim -15.9$ ppm/°C [15]. This would stimulate us to search new Mo-based ceramic systems for meeting the demands of LTCC technology.

In this communication, a new Mo-based dielectric ceramic of $La_2Zr_3(MoO_4)_9$ was reported. It exhibited a low synthesis temperature of 650 °C [16], particularly a low sintering temperature (< 800 °C) and desirable microwave dielectric properties. The phase crystal, sintering behavior, microstructure and microwave dielectric properties were systematically studied for the first time.

2. Experimental

The $La_2Zr_3(MoO_4)_9$ ceramics were synthesized by a conventional solid-state reaction method using high-purity starting powders of analytic-grade La_2O_3, ZrO_2 and MoO_3. The raw materials were weighed in stoichiometric amounts and then ball-milled for 4 h using zirconia balls and alcohol as the medium on a planetary milling machine. The resulting slurries were then rapidly dried and calcined at 650 °C for 6 h in air. The calcined powders were re-milled for 6 h and then mixed together with 5 wt% PVA as a binder. The granulated powders were subsequently pressed into cylinders with dimensions of 10 mm in diameter and 7–8 mm in height. The specimens were first heated at 550 °C in air for 4 h to remove the organic binder, and then sintered at 700 °C ~ 800 °C for 4 h.

The crystal structure of the fired ceramics was identified via an X-

* Corresponding author.
E-mail address: rzzuo@hotmail.com (R. Zuo).

http://dx.doi.org/10.1016/j.jeurceramsoc.2017.08.023
Received 2 July 2017; Received in revised form 4 August 2017; Accepted 16 August 2017

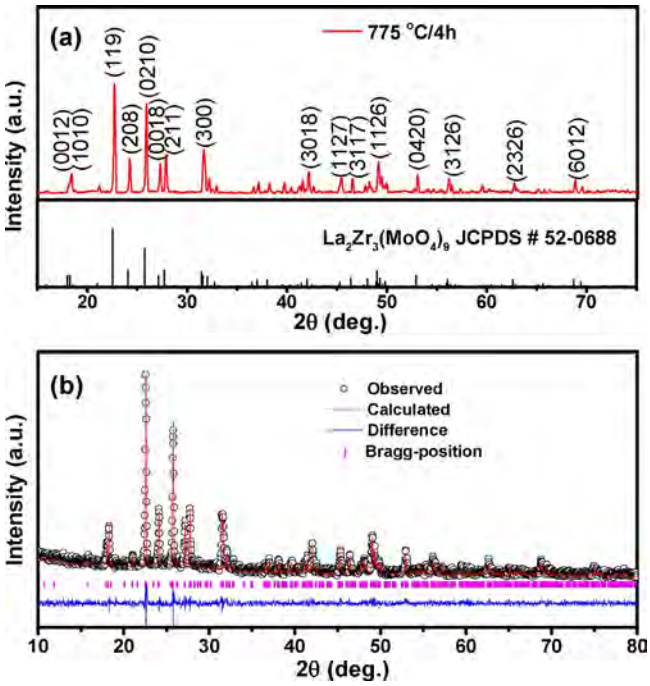

Fig. 1. (a) The XRD pattern and (b) the Rietveld refinement plot of $La_2Zr_3(MoO_4)_9$ ceramics sintered at 775 °C for 4 h.

ray diffractometer (XRD, D/Max2500 V, Rigaku, Japan) using Cu*Kα* radiation. The structural parameters were obtained from Rietveld refinement of the XRD data using the GSAS-EXPGUI program. The bulk densities of the sintered ceramics were measured by the Archimedes method. The microstructure of the specimens was observed using a field-emission scanning electron microscope (FE-SEM; SU8020, JEOL, Tokyo, Japan). Microwave dielectric properties of the sintered ceramics were measured using a network analyzer (N5230C, Agilent, Palo Alto, CA) and a temperature chamber (GDW-100, Saiweisi, Changzhou, China). The τ_f values of the samples were measured in the temperature range of 20 ~ 80 °C and calculated by the following equation:

$$\tau_f = \frac{f_2 - f_1}{f_1(T_2 - T_1)} \quad (1)$$

where f_1 and f_2 represent the resonant frequencies at T_1 and T_2, respectively.

3. Results and discussion

Fig. 1(a) presents the XRD pattern of $La_2Zr_3(MoO_4)_9$ ceramics sintered at 775 °C for 4 h. All the diffraction peaks matched well with the standard pattern of $La_2Zr_3(MoO_4)_9$ (JCPDS No. 52-0688) and no secondary phase was detected, indicating the formation of pure-phase $La_2Zr_3(MoO_4)_9$. To further understand its structure, Rietveld refinements were carried out by using GSAS software, in which a structural model of $Nd_2Zr_3(MoO_4)_9$ was used [17]. The refined plot of the sample sintered at 775 °C was selected as a representative, as shown in Fig. 1(b). The lattice parameters, cell volume and reliability factors of R_{wp}, R_p, and χ^2 for all studied samples after the Rietveld refinement are listed in Table 1. The R_{wp}, R_p, and χ^2 values were found to be in the range of 7–10%, 5–8%, and 1.8–2.1, respectively, indicating that the structural model is valid and the refinement result is reliable. Moreover, these crystal structure parameters are similar to those in a previous report [18]. With increasing sintering temperature, no systematic variation could be observed in lattice parameters, but the cell volume firstly decreased to the minimum at 775 °C and then kept almost constant with further increasing sintering temperature in the studied temperature range. Fig. 2(a,b) show the structure illustrations of

Table 1
Refined unit cell volume, reliability factors and good-of-fit indicator of $La_2Zr_3(MoO_4)_9$ ceramics at different sintering temperatures.

S.T. (°C)	a = b (Å)	c (Å)	Unit cell volume (Å^3)	R_{wp} (%)	R_p (%)	χ^2
700 °C	4.9483(3)	59.142 (2)	4966.6(3)	7.51	5.87	2.041
725 °C	4.8447(3)	59.123 (2)	4962.4(3)	7.66	6.03	2.035
750 °C	4.9425(5)	59.119 (4)	4959.9(6)	9.50	7.57	1.962
775 °C	4.9431(3)	59.104 (2)	4959.2(4)	7.05	5.56	1.822
800 °C	4.9417(3)	59.123 (2)	4959.4(4)	7.56	5.95	2.017

S.T.: sintering temperature; R_{wp}: the reliability factor of weighted patterns; R_p: the reliability factor of patterns; χ^2 goodness-of-fit indicator = $(R_{wp}/R_{exp})^2$.

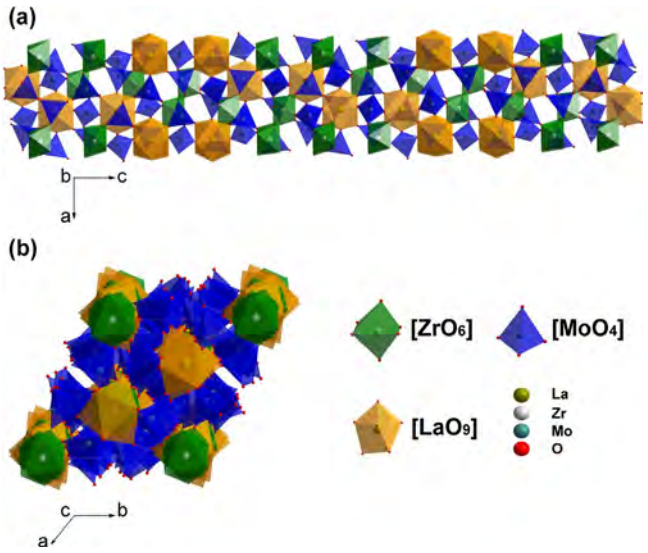

Fig. 2. The schematic crystal structure of $La_2Zr_3(MoO_4)_9$ seen along (a) a-axis and (b) c-axis.

$La_2Zr_3(MoO_4)_9$ seen along a-axis and c-axis, respectively. It can be seen that the La, Zr and Mo atoms are located at oxygen polyhedral sites with 9, 6 and 4-fold coordination, respectively. The LaO_9 polyhedra and ZrO_6 octahedra are linked to each other by their common oxygen vertices of the bridging MoO_3 tetrahedra of two sorts to form a three-dimensional mixed framework. In short, the $La_2Zr_3(MoO_4)_9$ structure can be viewed as interconnected polyhedrons with shared oxygen atoms at the vertices.

Fig. 3 shows the SEM images of $La_2Zr_3(MoO_4)_9$ ceramics sintered at different temperatures for 4 h. It can be observed that $La_2Zr_3(MoO_4)_9$ ceramics could be well sintered within the temperature range of 725–800 °C, and all the samples exhibited dense microstructure with identifiable grain boundaries. In addition, the grain size slightly increased with increasing sintering temperature. A more uniform microstructure with closely packed polygonal grains (~0.9 μm in average) was obtained in the sample sintered at 775 °C.

Fig. 4 shows the variation of relative density and ε_r of $La_2Zr_3(MoO_4)_9$ ceramics as a function of sintering temperature. It is obvious that all samples exhibited high relative densities (> 95%), keeping consistent with the microstructure observation. With the increase of sintering temperature, the relative density of $La_2Zr_3(MoO_4)_9$ ceramics firstly increased to a maximum approximately at 775 °C, and then decreased slightly with further increasing the sintering temperature (see Fig. 4(a)). ε_r also increased to the maximum of ~10.8 at 775 °C and decreased afterwards with increasing sintering temperature. The same variation in ε_r and relative density with sintering temperature indicated that density was the primary affecting factor of ε_r in current $La_2Zr_3(MoO_4)_9$ ceramics. In order to eliminate the influence of porosity on ε_r, the Bosman and Having's correction was applied to amend the ε_r

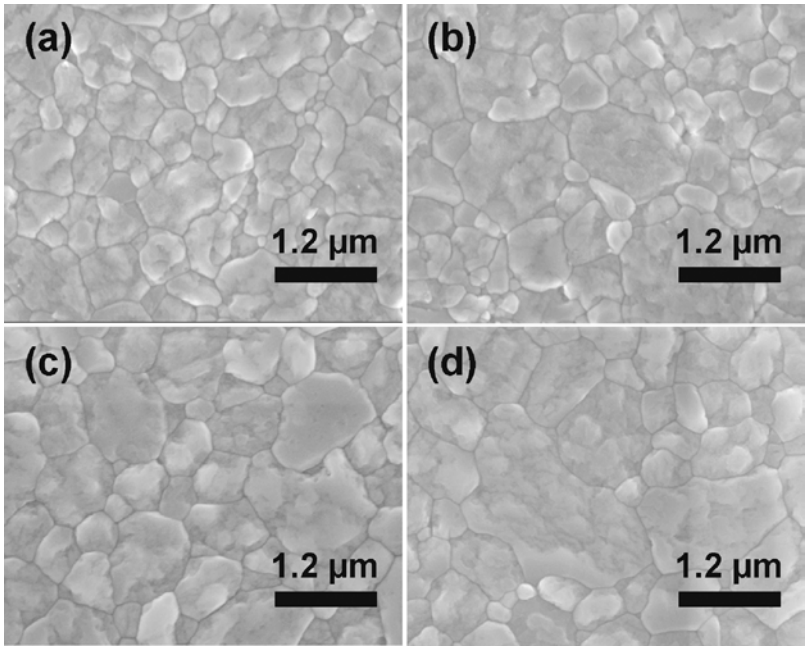

Fig. 3. SEM images on the polished and thermally etched surfaces of $La_2Zr_3(MoO_4)_9$ ceramics sintered at different temperatures for 4 h: (a) 725 °C, (b) 750 °C, (c) 775 °C, and (d) 800 °C.

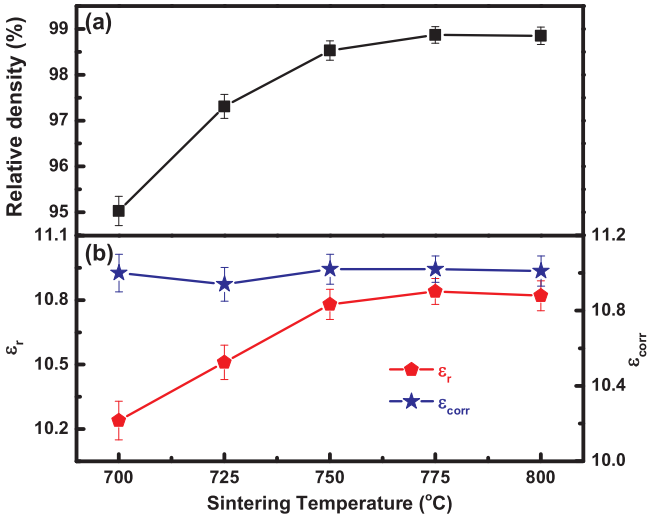

Fig. 4. The variation of (a) relative density and (b) permittivity of $La_2Zr_3(MoO_4)_9$ ceramics as a function of sintering temperature.

values of $La_2Zr_3(MoO_4)_9$ ceramics, as expressed by the following equation [19]:

$$\varepsilon_{corr} = \varepsilon_m (1 + 1.5p) \quad (2)$$

where p is the fractional porosity, ε_{corr} and ε_m are the corrected and measured values of the permittivity, respectively. The variation of ε_{corr} as a function of sintering temperature is also shown in Fig. 4(b). As expected, the ε_{corr} values were almost identical in the whole sintering temperature range, which were slightly higher than ε_m values. The ε_{corr} value (~11.0) was very close to the ε_m value (~10.8) for the sample sintered at 775 °C. Besides, the theoretical permittivity (ε_{th}) also can be predicted by using the Clausius-Mosotti equation [20]:

$$\varepsilon_{th} = \frac{3V_m + 8\pi\alpha_D^T}{3V_m - 4\pi\alpha_D^T} \quad (3)$$

where b is a constant ($4\pi/3$), α_D^T and V_m represent the sum of polarizability of constituent ions, and the molecular volume, respectively. However, the ε_{th} is about 1.35 for the sample sintered at 775 °C. Such a big deviation between ε_{th} and ε_m might be related to the inaccurate α_D^T for the poor additivity relationship in molybdates as highlighted by Shannon [20]. Similar phenomenon also occurred in other systems [21].

The variation of Qxf in $La_2Zr_3(MoO_4)_9$ ceramics as a function of sintering temperature is shown in Fig. 5(a). In general, the dielectric loss can be divided into extrinsic loss and intrinsic loss. The extrinsic loss is mainly caused by density, secondary phase, grain size and lattice defects, while the intrinsic loss is mainly caused by structure characteristics. In current work, all samples possessed a high density (> 95%), so the effect of extrinsic factors could be neglected. Therefore, the structure characteristics should be the dominant factors that influence Qxf values, as evaluated by the packing fraction (f) defined by the summation of the volume of packed ions (V_{PI}) over the volume of a primitive unit cell (V_{PUC}). It can be expressed by the following equation [22]:

$$f(\%) = \frac{V_{PI}}{V_{PUC}} xZ \quad (4)$$

where Z is the number of molecule per unit cell. The calculated packing fraction of $La_2Zr_3(MoO_4)_9$ ceramics is also presented in Fig. 5(a). The

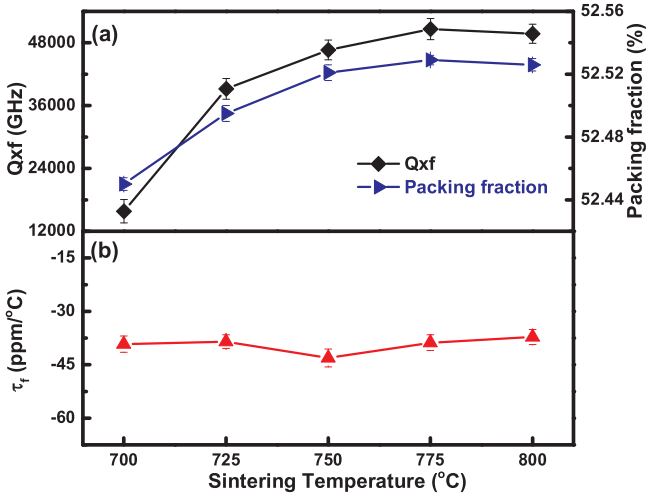

Fig. 5. The variation of (a) Qxf and packing fraction, and (b) τ_f of $La_2Zr_3(MoO_4)_9$ ceramics as a function of sintering temperature.

variation of Qxf as a function of sintering temperature is consistent with that of packing fraction, meaning the close dependence of Qxf value on packing fraction. Fig. 5(b) shows the variation of τ_f values of $La_2Zr_3(MoO_4)_9$ ceramics at different sintering temperatures. It can be seen that the τ_f values remained around -38 ppm/°C mainly because the crystal structure was almost unchanged.

4. Conclusions

In this work, a novel low-temperature fired microwave dielectric ceramic $La_2Zr_3(MoO_4)_9$ was successfully prepared by a solid-state reaction method. The results indicated that the $La_2Zr_3(MoO_4)_9$ ceramic belonged to a trigonal system with space group $R\bar{3}c$. Highly compact ceramics with a high relative density of above 95% could be obtained at a relatively low temperature of below 800 °C. Excellent microwave dielectric properties of $\varepsilon_r \sim 10.8$, Qxf ~ 50,628 GHz (at 10.45 GHz), and $\tau_f \sim -38.8$ ppm/°C could be achieved for the sample sintered at 775 °C for 4 h.

Acknowledgement

Financial support from the Anhui Provincial Natural Science Foundation (1508085JGD04) is gratefully acknowledged.

References

[1] M.T. Sebastian, H. Jantunen, Low loss dielectric materials for LTCC applications: a review, Int. Mater. Rev. 53 (2008) 57–90.
[2] M. Valant, D. Suvorov, Chemical compatibility between silver electrodes and low-firing binary-oxide compounds: conceptual study, J. Am. Ceram. Soc. 83 (2000) 2721–2729.
[3] S. Kawashima, N. Nishida, I. Ueda, H. Ouchi, $Ba(Zn_{1/3}Ta_{2/3})O_3$ ceramics with low dielectric loss at microwave-frequencies, J. Am. Ceram. Soc. 66 (1983) 241–243.
[4] K. Matsumoto, T. Hiuga, K. Takada, H. Ichimura, $Ba(Mg_{1/3}Ta_{2/3})O_3$ ceramics with ultra-low loss at microwave-frequencies, IEEE Trans. Ultrason. Ferroelectr. Freq. Control 33 (1986) 118–121.
[5] D. Zhou, H. Wang, L.X. Pang, C.A. Randall, X. Yao, Bi_2O_3-MoO_3 binary system: an alternative ultralow sintering temperature microwave dielectric, J. Am. Ceram. Soc. 92 (2009) 2242–2246.
[6] D. Zhou, L.X. Pang, H. Wang, X. Yao, Low temperature firing microwave dielectric ceramics $(K_{0.5}Ln_{0.5})MoO_4$ (Ln = Nd and Sm) with low dielectric loss, J. Eur. Ceram. Soc. 31 (2011) 2749–2752.
[7] U. Došler, M.M. Kržmanc, B. Jančar, D. Suvorov, A high-Q microwave dielectric material based on $Mg_3B_2O_6$, J. Am. Ceram. Soc. 93 (2010) 3788–3792.
[8] Y.P. Liu, Y.N. Wang, Y.M. Li, J.J. Bian, Low temperature sintering and microwave dielectric properties of $LiMBO_3$ (M = Ca, Sr) ceramics, Ceram. Int. 42 (2016) 6475–6479.
[9] L. Fang, H.H. Guo, W.S. Fang, Z.H. Wei, C.C. Li, $BaTa_2V_2O_{11}$: a novel low fired microwave dielectric ceramic, J. Eur. Ceram. Soc. 35 (2015) 3765–3770.
[10] Y. Wang, R.Z. Zuo, C. Zhang, J. Zhang, T.W. Zhang, Low-temperature-fired $ReVO_4$ (Re = La, Ce) microwave dielectric ceramics, J. Am. Ceram. Soc. 98 (2015) 1–4.
[11] L.X. Pang, D. Zhou, Z.M. Qi, W.G. Liu, Z.X. Yue, I.M. Reaney, Structure-property relationships of low sintering temperature scheelite-structured (1-x)$BiVO_4$-x$LaNbO_4$ microwave dielectric ceramics, J. Mater. Chem. C 5 (2017) 2695–2701.
[12] D. Zhou, D. Guo, W.B. Li, L.X. Pang, X. Yao, D.W. Wang, I.M. Reaney, Novel temperature stable high-ε_r microwave dielectrics in the Bi_2O_3-TiO_2-V_2O_5 system, J. Mater. Chem. C 4 (2016) 5357–5362.
[13] L.X. Pang, D. Zhou, W.B. Li, Z.X. Yue, High quality microwave dielectric ceramic sintered at extreme-low temperature below 200 °C and co-firing with base metal, J. Eur. Ceram. Soc. 37 (2017) 3073–3077.
[14] H.H. Xi, D. Zhou, B. He, H.D. Xie, Microwave dielectric properties of scheelite structured $PbMoO_4$ ceramic with ultralow sintering temperature, J. Am. Ceram. Soc. 97 (2014) 1375–1378.
[15] X.L. Zhai, X. Zheng, H.H. Xi, W.B. Li, J. Han, D. Zhou, Microwave dielectric properties of $LiKSm_2(MoO_4)_4$ ceramics with ultralow sintering temperatures, J. Am. Ceram. Soc. 98 (2015) 2716–2719.
[16] F. Baur, T. Jüstel, New red-emitting phosphor $La_2Zr_3(MoO_4)_9$: Eu^{3+} and the influence of host absorption on its luminescence efficiency, Aust. J. Chem. 68 (2015) 1727–1734.
[17] R.F. Klevtsova, S.F. Solodovnikov, Y.L. Tushinova, B.G. Bazarov, L.A. Glinskaya, Z.G. Bazarova, A new type of mixed framework in the crystal structure of binary molybdate $Nd_2Zr_3(MoO_4)_9$, J. Struct. Chem. 41 (2000) 280–284.
[18] S. Qi, Y. Huang, H. Cheng, H.J. Seo, Luminescence and application of red-emitting phosphors of Eu^{3+} activated $R_2Zr_3(MoO_4)_9$ (R = La, Sm Gd), Electron. Mater. Lett. 12 (2016) 171–177.
[19] A.J. Bosman, E.E. Havinga, Temperature dependence of dielectric constants of cubic ionic compounds, Phys. Rev. 129 (1963) 1593–1600.
[20] R.D. Shannon, Dielectric polarizabilities of ions in oxides and fluorides, J. Appl. Phys. 73 (1993) 348–366.
[21] D. Zhou, L.X. Pang, H.D. Xie, J. Guo, B. He, Z.M. Qi, T. Shao, X. Yao, C.A. Randall, Crystal structure and microwave dielectric properties of an ultralow-temperature-fired $(AgBi)_{0.5}WO_4$ ceramic, Eur. J. Inorg. Chem. 2 (2014) 296–301.
[22] J. Li, C.C. Li, Z.H. Wei, Y. Tang, C.X. Su, L. Fang, Microwave dielectric properties of a low-firing $Ba_2BiV_3O_{11}$ ceramic, J. Am. Ceram. Soc. 98 (2015) 683–686.